SF2A 2016
C. Reylé, J. Richard, L. Cambrésy, M. Deleuil, E. Pécontal, L. Tresse and I. Vauglin (eds)

MODELING THE REVERBERATION OF OPTICAL POLARIZATION IN AGN

P. A. Rojas Lobos[1], R. Goosmann[1] and F. Marin[1]

Abstract. According to the standard paradigm, the strong and compact luminosity of active galactic nuclei (AGN) is due to multi-temperature black body emission originating from an accretion disk formed around a supermassive black hole. This central engine is thought to be surrounded by a dusty region along the equatorial plane and by ionized winds along the poles. The innermost regions cannot yet be resolved neither in the optical nor in the infrared and it is fair to say that we still lack a satisfactory understanding of the physical processes, geometry and composition of the central (sub-parsec) components of AGN. Like spectral or polarimetric observations, the reverberation data needs to be modeled in order to infer constraints on the AGN geometry (such as the inner radius or the half-opening angle of the dusty torus). In this research note, we present preliminary modeling results using a time-dependent Monte Carlo method to solve the radiative transfer in a simplified AGN set up. We investigate different model configurations using both polarization and time lags and find a high dependency on the geometry to the time-lag response. For all models there is a clear distinction between edge-on or face-on viewing angles for fluxes and time lags, the later showing a higher wavelength-dependence than the former. Time lags, polarization and fluxes point toward a clear dichotomy between the different inclinations of AGN, a method that could help us to determine the true orientation of the nucleus in Seyfert galaxies.

Keywords: Galaxies: active, galaxies: nuclei, polarization, radiative transfer

1 Introduction

Active galactic nuclei (AGN) are the strongest steady sources in the Universe. While being extremely spatially compact, they produce enough bolometric luminosity to eventually outshine their host galaxy. It is an accepted paradigm that such strong and compact emission is due to accretion onto a supermassive black hole (SMBH, Salpeter 1964; Lynden-Bell 1969). In thermal, radio-quiet AGN the SMBH is surrounded by an accretion disk producing the optical and UV continuum radiation (see Shields 1978, Shakura and Sunyaev 1973 and Pringle, Rees and Pacholczyk 1973). This emission is reprocessed by other structures surrounding the disk, such as the so-called broad line emission region (BLR), or a circumnuclear dusty medium often called the "dusty torus" (Antonucci 1993). This dusty region extends to a spatial scale of a few parsecs for a $10^7 M_\odot$ SMBH, but only in very few objects the circumnuclear dust is barely resolvable by near-IR interferometry techniques. The innermost parts cannot yet be resolved neither in the optical nor the infrared and it is fair to say that we still lack a satisfactory understanding of the physical processes, geometry and composition of the central (sub-parsec) components of AGN.

Both, the BLR and the dusty torus are somewhat confined to the equatorial plane that is defined by the accretion disk. The dusty torus is opaque to optical light (Gaskell 2009) and therefore obscures the BLR at all lines of sight intercepting it. Observers at such equatorial viewing angles do not see broad optical emission lines and therefore observe a so-called type-2 AGN. At polar viewing angles, the BLR is visible and the optical spectrum denotes a type-1 object. This is a fundamental axis of the so-called Unified Model of AGN that attempts to explain the observational diversity of active galaxies as an orientation effect. To verify this scenario the role of polarimetry was crucial. Antonucci (1984) and Antonucci and Miller (1985) observed polarized broad lines in highly inclined Seyfert galaxies and found a relation between low inclination (type-1) and high-inclination sources (type-2). They thus postulated that both AGN types share the same morphology but are

[1] Observatoire Astronomique de Strasbourg, Université de Strasbourg, CNRS, UMR 7550, 11 rue de l'Université, 67000 Strasbourg, France

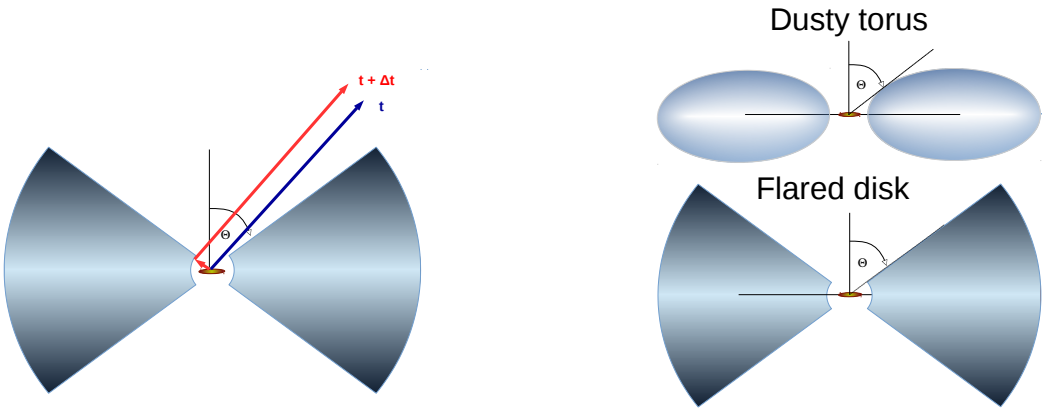

Fig. 1: Left: Reverberation principle – the blue line traces unpolarized photons coming directly from the source. The red line shows photons scattered inside the equatorial scattering region (polarized light). Right: model geometries – the doughnut-shaped torus (top) and the extended flared-disk geometry (bottom).

seen at a different system inclination. Since then, a lot of effort has been put into understanding the complex polarization signal observed in the optical band. In particular, Smith et al. (2004) suggested that a flattened equatorial scattering region could explain the specific polarization observed in type-1 AGN: a low polarization degree P (inferior to 1% in most of the cases) associated with a polarization position angle parallel to the symmetry axis of the circumnuclear dust region. It was shown by our collaboration that also a wide half opening angle of the dusty torus produces the polarization characteristics of type-1 AGN Marin et al (2012).

Knowing that flattened scattering regions in type-1 AGN produce continuum polarization should make it possible to conduct polarization reverberation mapping as introduced by Gaskell et al. (2012). The reverberation lag is due to a difference in light travel time between continuum radiation coming directly from the accretion disk and scattered radiation coming from structures farther away (e.g., from the torus, see Fig. 1, left). It is obtained by cross-correlating the optical continuum lightcurve with the polarized spectrum. The latter is obtained by multiplying the polarization fraction with the spectral intensity. The polarized time lag holds information on the average distance between the continuum source and the scattering regions. In this way, Gaskell et al. (2012) were able to infer the size of the inner scattering regions in the Seyfert-1 galaxy NGC 4151.

Like spectral or polarimetric observations, the reverberation data needs to be accurately modeled to infer constraints on the AGN geometry (such as the inner radius or the half-opening angle of the dusty torus). In this research note, we present preliminary modeling results using a time-dependent Monte Carlo method to solve the radiative transfer in a simplified AGN set up. We present results for polarization and time lags assuming different model configurations.

2 Modeling the circumnuclear region

The STOKES code is a Monte-Carlo radiative transfer code written by Goosmann and Gaskell (2007), Marin et al (2012) and Marin, Goosmann and Gaskell (2015) that computes the Stokes parameters of light, from which we can derive the polarization percentage, position angle, and total flux. In its latest public version, it also stores the time information in order to compute time-lags. The code allows the user to define different geometries and opacities for emission and scattering structures around a set of emitting regions. A free-to-download version of the code (v1.2 at this moment) can be found at: http://www.stokes-program.info/ . A recent review of the code performance is given in Marin & Goosmann (2014).

To investigate how polarized reverberation mapping can improve our knowledge of the morphology and composition of the dusty region at the center of AGN, we constructed a toy-model representative of the inner few parsecs of a Seyfert galaxy. At the center of the model, we implemented an irradiating continuum source using an isotropic point-like region emitting an unpolarized flux according to a power-law spectrum $F_* \propto \nu^\alpha$ with $\alpha = 1$. Around it we defined a flattened dust distribution that could take two distinct forms: either a flared-disk or an elliptically-shaped torus. An illustration of the two geometries can be seen in Fig. 1 (right). The filling of the equatorial region was either uniform (volume filling factor equal to unity) or non-uniform, i.e.

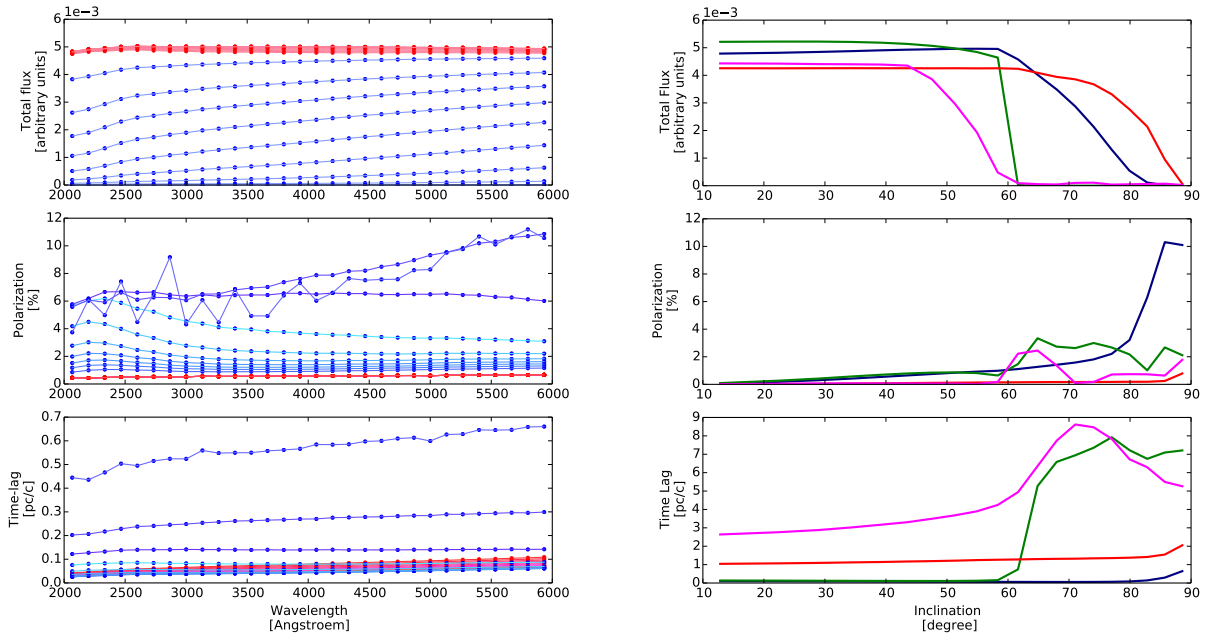

Fig. 2: Total flux (top), polarization percentage (middle) and time lag (bottom). The red dots show viewing angles lower than 60° (type-1) and blue dots show viewing angles above 60° (type-2). Left: Plots as a function of wavelength (left) for a uniform-density torus. Right: V-band data as a function of the system inclination. Blue line: uniform-dusty-torus, green line: uniform-flared-disk, red line: clumpy-dusty-torus, magenta line: clumpy-flared-disk.

clumpy (volume filling factor = 25). For all models, we considered the same torus dimensions: distance from the center: 0.0067 pc, external radius: 15.0067 pc, and inclination angle: 30° from the symmetry axis. The inner radius was set according to the time lag of 8 light-days found by Gaskell et al. (2012) for NGC 4151. The outer torus radius and the half-opening angle are based on near-infrared polarimetric observations by Ruiz et al. (2003). The dusty region is optically thick, as is expected from observations with a total optical depth of ~ 150 along the observer's line-of-sight. Both models (flared-disk and toroidal geometries) were tested with two dust prescriptions: "AGN-dust" presented in Gaskell et al. (2004) and "MilkyWay-dust" ("MW-dust") as prescribed by Mathis, Rumpl & Nordsieck (1977). AGN-dust is composed of 85% silicate and 15% graphite; MW-dust is composed of 62.5% silicate and 37.5% graphite. The grain radius, a, varies from 0.005μm to 0.250μm following a distribution $n(a) \propto a^s$ with $s = -2.05$ for AGN and $s = -3.5$ for MW dust.

3 Results

We first study the case of a uniform-density torus. In Fig. 2 (left), we plot the spectral flux, polarization and time lag as a function of wavelength. The spectral results can be compared to earlier work given in (Goosmann and Gaskell 2007). It turns out that both the strong direct emission seen at type-1 viewing angles and the significantly weaker scattered emission seen at type-2 orientations are mostly independent of wavelength. A slight depression is seen below 3000 Å, which can be related to Mie scattering becoming more prominent versus Rayleigh scattering as well as to the presence of the dust-related 2175 Å feature. Apart from a similar variation in the near-UV and a slight overall rise towards longer wavelengths, the time lag is mostly insensitive to wavelength. This behavior is confirmed for the other modeling geometries studied in this work. Furthermore, it was discussed in (Goosmann and Gaskell 2007) that the polarization properties induced by dust scattering in toroidal geometries do not vary much with wavelength. Next, we focus on the results as a function of the system inclination (Fig. 2 right). It turns out that the time lag of the polarized emission is not affected when modifying the dust prescription. Thus, we only present modeling results for the case of standard "Milky Way" dust. A discussion on the dust prescription and polarization effects is given in Goosmann and Gaskell (2007).

The total flux and polarization as a function of inclination confirm what was shown in previous papers (Goosmann and Gaskell 2007; Marin et al 2012; Marin, Goosmann and Gaskell 2015). The flux must be much stronger at polar viewing angles (such as expected from type-1 AGN) than below the torus horizon (type-2) where only scattered radiation is seen. The scattered radiation is more strongly polarized but also accumulates a larger time lag. Notice that a time lag of zero corresponds to the direct emission from the source seen by the observer without any deviation. The fact that the time lag and the polarization fraction at type-1 inclinations are still larger than zero is due to the superimposed scattered component. At type-2 viewing angles the observed radiation must scatter inside the torus funnel before it escapes, increasing the time lag significantly.

The angular profile of the total flux, polarization and the time lag differ between the four geometries. We find a difference in the angular flux distribution between flared and toroidal shapes: the flared disk allows less radiation to be scatted towards type-2 viewing angles than the doughnut-shaped torus. A similar effect was found and discussed before when comparing the scattering properties between a large and a compact torus for the same half-opening angle (see section 4.2 and figure 7 in Goosmann and Gaskell 2007, for more details). For a given overall geometry, i.e. either flared or toroidal, the total flux and time lag are only in rough agreement with each other. Introducing clumpiness leads to a somewhat smoother and broader transition around the torus horizon and strongly lowers the polarization fraction and therefore the polarized flux.

4 Summary and conclusion

We modeled the polarization properties and time dependence of radiation scattered by circumnuclear dust in AGN. The inner radius of the dust region was fixed from polarization reverberation measurements in NGC 4151 (Gaskell et al. 2012). At type-1 viewing angles we find almost no variation in shape for all models, but we find a clear difference in the angular flux distribution depending on the geometry. Our results extend the work in Goosmann and Gaskell (2007) in terms of time lags.

There are additional differences in the polarization signature between a torus and a flared disk. While the torus models, either uniform or clumpy, do not show large differences in time-lag between type-1 or type-2 viewing angles, the case is different for flared geometries. The time lag is almost seven times larger at type-2 viewing angles than at polar inclinations. A flared disk structure leads to more important delays at edge-on inclinations, together with lower fluxes and polarization than for a toroidal dusty torus.

In conclusion, time-resolved polarimetry adds independent constrains to the unresolved structure of AGN and we aim to investigate in further detail these differences in a forthcoming paper.

This work was supported by CONICYT PFCHA/BecasCHILE Doctorado en el extranjero 72150573.

References

Antonucci, R. 1984, ApJ, 278, 499
Antonucci, R. 1993, ARA&A, 31, 473
Antonucci, R. and Miller, J.S., 1985, ApJ, 297, 621A
Gaskell, C. M., Goosmann, R. W., Antonucci, R. R. J., & Whysong, D., 2004, ApJ, 616, 147
Gaskell, C. M. 2009, NewAR 53, 140
Gaskell, C. M. and Goosmann, R. W. and Merkulova, N. I. and Shakhovskoy, N. M. and Shoji, M. 2012, ApJ, 749, 148
Goosmann, R. W.and Gaskell, C. M. 2007, A&A, 465, 129
Lynden-Bell, D. 1969, Nature 223, 690
Marin, M., Goosmann, R. W., Gaskell, C. M., Porquet, D. and Dovciak, M. 2012, A&A, 548, 121
Marin, F., & Goosmann, R. W. 2014, SF2A-2014: Proceedings of the Annual meeting of the French Society of Astronomy and Astrophysics, 103
Marin, F., Goosmann, R. W. and Gaskell, C. M. 2015, A&A, 577, 66
Mathis, J. S., Rumpl, W., & Nordsieck, K. H., 1977, ApJ, 217, 425
Pringle, J. E. and Rees, M. J. and Pacholczyk, A. G., 1973, A&A, 29, 179
Ruiz, M. and Young, S. and Packham, C. and Alexander, D. M. and Houghg, J. H. 2003, MNRAS, 340, 733R
Salpeter, E. E. 1964, ApJ, 140, 796
Shakura, N. I. And Sunyaev, R. A. 1973, A&A, 24, 337
Shields, G. A., 1978, Nature, 272, 706
Smith, J. E. et al., 2004, MNRS, 350, 1405